

# Naked active galactic nuclei

M.R.S. Hawkins<sup>1</sup>

Institute for Astronomy (IfA), University of Edinburgh, Royal Observatory, Blackford Hill, Edinburgh EH9 3HJ  
e-mail: mrsh@roe.ac.uk

Received April 21, 2004; accepted May 29, 2004

**Abstract.** In this paper we report the discovery of a new class of active galactic nucleus in which although the nucleus is viewed directly, no broad emission lines are present. The results are based on a survey for AGN in which a sample of about 800 quasars and emission line galaxies were monitored yearly for 25 years. Among the emission line galaxies was the expected population of Seyfert 2 galaxies with only narrow forbidden lines in emission, and no broad lines. However, from the long term monitoring programme it was clear that some 10% of these were strongly variable with strong continuum emission. It is argued that these objects can only be Seyfert 1 galaxies in which the nucleus is viewed directly, but in which broad emission lines are completely absent. We compare these observations with other cases from the literature where the broad line region is reported to be weak or variable, and investigate the possibility that the absence of the broad line component is due to reddening. We conclude that this does not account for the observations, and that in these AGN the broad line region is absent. We also tentatively identify more luminous quasars from our sample where the broad emission lines also appear to be absent. The consequences of this for AGN models are discussed, and a case is made that we are seeing AGN in a transition stage between the fuel supply from a surrounding star cluster being cut off, and the nucleus becoming dormant.

**Key words.** quasars: general – galaxies: active

## 1. Introduction

The diverse phenonema which characterise the class of objects known as Active Galactic Nuclei (AGN) have been reconciled in a unified scheme (Antonucci 1993) in which viewing angle plays a crucial role in the observed properties of the system. An important feature of the unified model is the distinction between Seyfert 1 galaxies and quasars where the active nucleus is viewed directly, along with emission from fast moving gas clouds surrounding it, and Seyfert 2 galaxies where this central region is hidden from view by a dusty torus. Although there is some difference in the observed velocity structure in the clouds, they are taken to be a fundamental feature of AGN.

From an observational point of view, there is a clear distinction between Seyfert 1 and 2 galaxies. The spectra of Seyfert 1 galaxies show broad emission lines with a velocity dispersion of around 6000 to 10,000 km sec<sup>-1</sup> together with narrow relatively weak forbidden and permitted lines. The narrow lines typically have a velocity dispersion of less than 1000 km sec<sup>-1</sup>, and a [O III]  $\lambda$ 5007/H $\beta$  ratio around 10. In addition, Seyfert 1 galaxies have a strong variable component of continuum emission from the active nucleus, whereas for Seyfert 2 galaxies where the nucleus is obscured, only a faint reflection of the nucleus is seen in polarised light (Crenshaw & Kraemer 2000). Most Seyfert galaxies fit comfortably into one or other of these classes, consistent with predictions from the unified scheme.

The unified scheme incorporates the idea that all AGN have a broad line region (BLR) which would be visible but for the obscuring torus. However, the place of the broad line region in the evolution of AGN is far from clear, and the possibility that some AGN may not contain a BLR has not been ruled out. There are a number of interesting departures from the norm, the most prominent of which is a class of ‘narrow line’ Seyfert 1 galaxies (Osterbrock & Pogge 1985, Rodríguez-Ardila et al. 2000). In these AGN the emission lines are less broad than normal, in extreme cases with a width close to the forbidden lines from the narrow line region, but they are always strong, with a [O III]  $\lambda$ 5007/H $\beta$  ratio less than 3. There are also other situations where emission lines are very weak. For example there are a number of quasars where the Lyman- $\alpha$  line appears to be cut away to a thin spike by absorption, and in one notable case (Fan et al. 1999) appears to be absent altogether. Another interesting example (McDowell et al. 1995) is PG 1407+265 with H $\beta$  and Lyman- $\alpha$  very weak, but a strong broad H $\alpha$  line. Emission line strengths are also known to vary strongly in some Seyfert 1 galaxies, apparently in response to changes in the brightness of the continuum.

NGC 4151 provides a good example (Clavel et al. 1987), but the broad lines by no means disappear, the C IV  $\lambda 1550$  line changing in width between 2600 and 5500 km s<sup>-1</sup> as the continuum brightness varies. Lastly it is worth mentioning the long sought class of type 2 quasar. These are luminous counterparts of Seyfert 2 galaxies, and were expected to exist on the basis of the unified model. Some good examples are now known (Norman C. et al. 2002), and apart from their luminosity (at  $M_R \sim -23$ ) they have properties closely resembling Seyfert 2 galaxies. They have virtually no continuum emission, and most of their observed flux comes from strong narrow forbidden lines. It is clear that in these objects we are not looking directly at the nucleus, which is obscured by a dusty torus as for Seyfert 2 galaxies.

In this paper we report the discovery of a new class of AGN where the high velocity clouds are completely absent, although the nucleus is viewed directly, unobscured by the torus. These naked AGN have the spectral properties of Seyfert 2 galaxies, with the exception that they have a strong variable continuum implying that we are seeing the active nucleus directly. This result is discussed in the context of current AGN models.

## 2. The Seyfert galaxy survey

### 2.1. Sample selection

Over the last 25 years a large-scale monitoring programme for AGN has been carried out with a view to characterising the nature of the optical variations and putting constraints on the structure of the accretion disc (Hawkins 1996, Hawkins 2000, Hawkins 2002, Hawkins 2003). The survey is based on a long series of photographic plates from the UK 1.2m Schmidt telescope in Australia, measured with the COSMOS and SuperCOSMOS measuring machines at Edinburgh. The survey area comprises the central 20 deg<sup>2</sup> of the ESO/SERC field 287 centred on 21h 28m, -45° (1950) and plates were taken every year from 1977 to 2002 in the  $B_J$  passband (IIIa-J emulsion with a GG395 filter). Extensive coverage was also obtained in other passbands allowing AGN to be selected on the basis of colour and variability (Hawkins 2000).

The measurement of the photographic plates provided a catalogue of some 200,000 objects in the 20 deg<sup>2</sup> area, together with UBVRI colours. There were also yearly measurements in  $B_J$  going back to 1977. Candidate AGN for follow-up were selected from this catalogue on the basis of their blue colour ( $(U - B) < 0$ ) or variability according to the criteria given in Hawkins (1996). This effectively required that the amplitude of variation exceeded 0.4 magnitudes. In all, around 1500 candidates down to a magnitude limit of  $B_J < 21.5$  were selected as AGN candidates for follow-up spectroscopic study.

### 2.2. Spectroscopy

The main purpose of the spectroscopic follow-up was to confirm the identity of the candidates as AGN, and obtain redshifts. Given the high surface density of candidates, the ideal instrument for this purpose was the 2dF multi-fibre spectrograph on the Anglo Australian Telescope at Siding Spring. In a 4 night run in July 2002, 1400 AGN candidates were observed in 5 separate pointings making up an area of about 12 deg<sup>2</sup> and including some overlap. All spectra were reduced using standard 2dF software to provide instrumental and wavelength calibration, and also sky subtraction. The feasibility of flux calibrating 2dF data is somewhat controversial, and has presented problems to other groups (Croom et al. 2002). However, in the region of interest of the spectra discussed here, the response function is essentially flat, and the sensitivity only starts to decline shortward of about 4500 Å. This is well clear of any redshifted H $\beta$  lines which are the principal features of interest in this paper. On this basis it was decided that to introduce a controversial procedure in a situation where the results of the analysis would not be affected by its inclusion would be to add an unnecessary complication to the line of argument. Consequently, all spectra illustrated in this paper are shown without flux calibration.

Redshifts for all emission line objects were measured with the FIGARO package. Of the 894 candidates with successfully measured redshifts, 129 were found to have emission line spectra with redshift  $z < 0.5$ , and these were used to form a catalogue of candidate Seyfert galaxies. To determine a more precise classification for these low redshift objects, the spectra were re-analysed with a view to measuring line widths and line ratios. To do this, the Gaussian fitting routine in FIGARO was used. This routine gives as outputs the fitted line centre, full width at half maximum (FWHM) and line integral. Although the routine outputs error estimates for each measurement based primarily on photon statistics, these were checked by comparing duplicate measures of the same object and of skylines. The calculated errors from the FIGARO package were found to be too low, and so the empirically determined errors were used. These amounted to approximately 0.6 Å or 30 km sec<sup>-1</sup>. The spectral resolution as measured from the sky lines was 10.4 Å or 520 km sec<sup>-1</sup> at 6000 Å.

The measurement of line integrals for the purposes of obtaining line ratios is well known to be problematic as a number of effects, both cosmological and instrumental, can cause problems. In the case of 2dF data the instrumental effects are especially troublesome, as accurate sky subtraction is hard to achieve, and flux calibration is unreliable. The normal way around these problems is to measure line ratios of lines of similar wavelength when systematic effects largely cancel out, and this is the approach we adopt in this paper. The line ratio of principal interest here is [O III]  $\lambda 5007$ /H $\beta$  where the error determined from repeat measures of the same object was  $\pm 5\%$ .

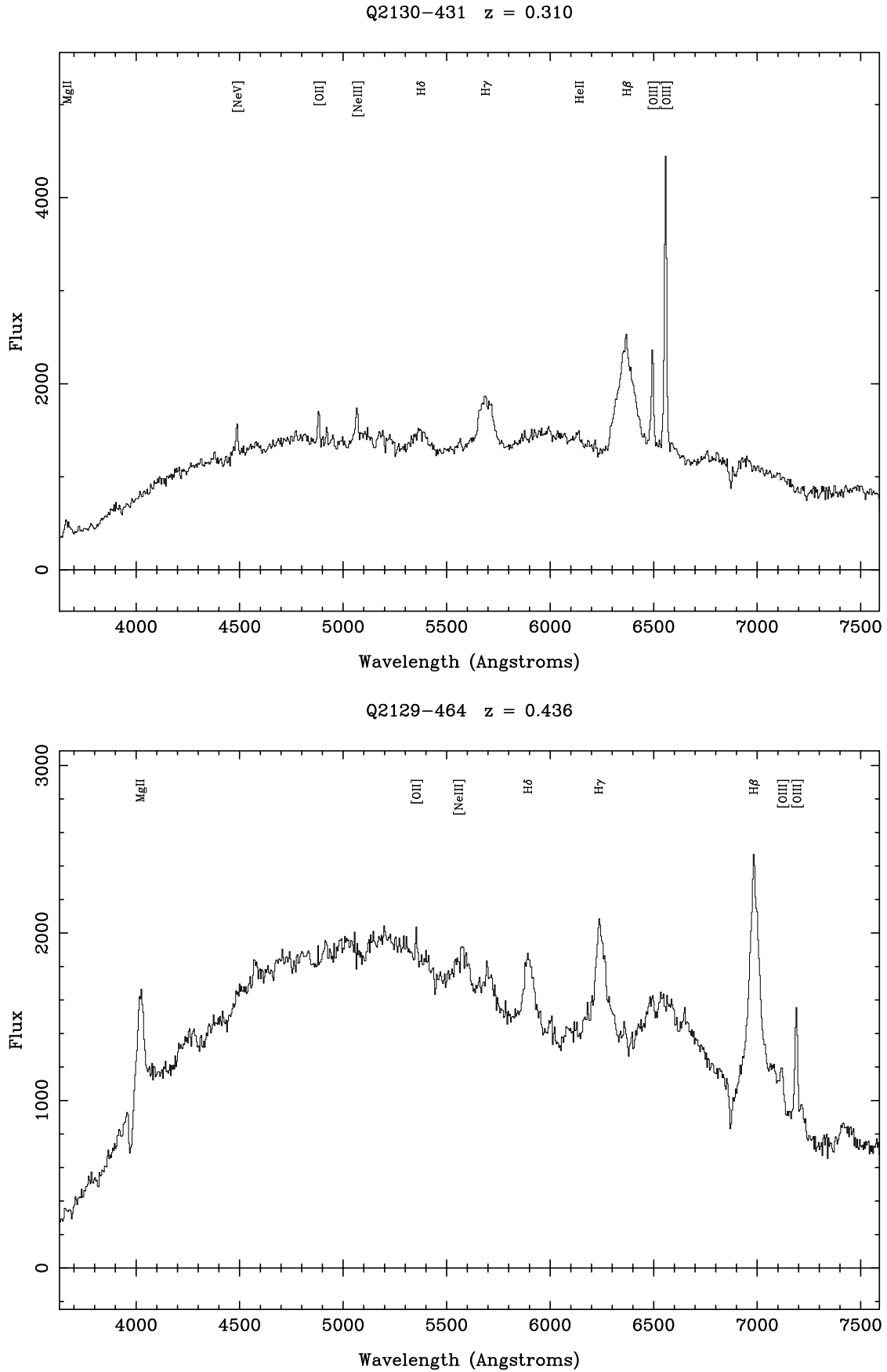


**Fig. 1.** Spectra of typical Seyfert 1 galaxies (flux in arbitrary units).

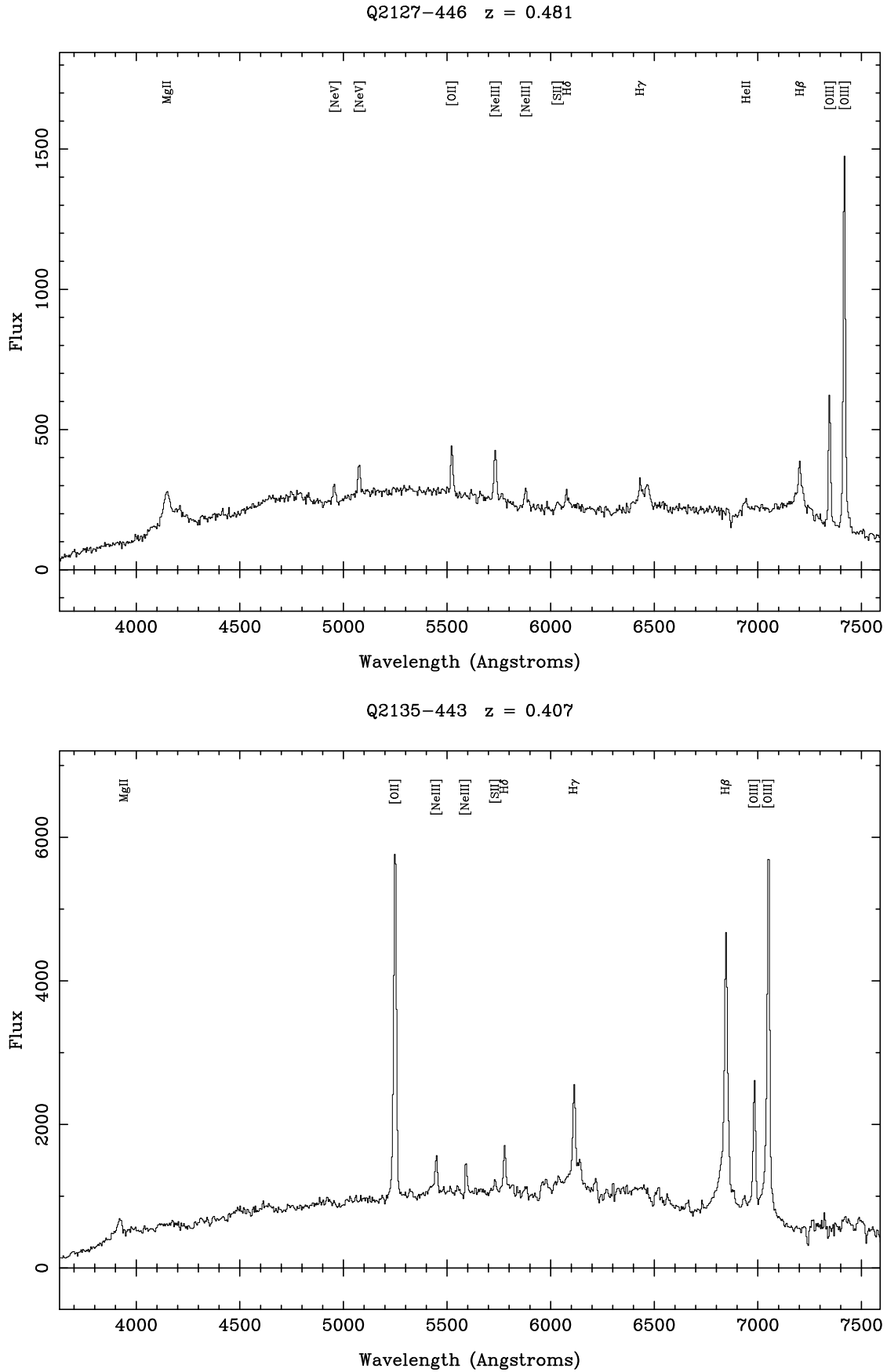


**Fig. 2.** Spectra of typical narrow line Seyfert 1 galaxy (top) and LINER (bottom) (flux in arbitrary units).

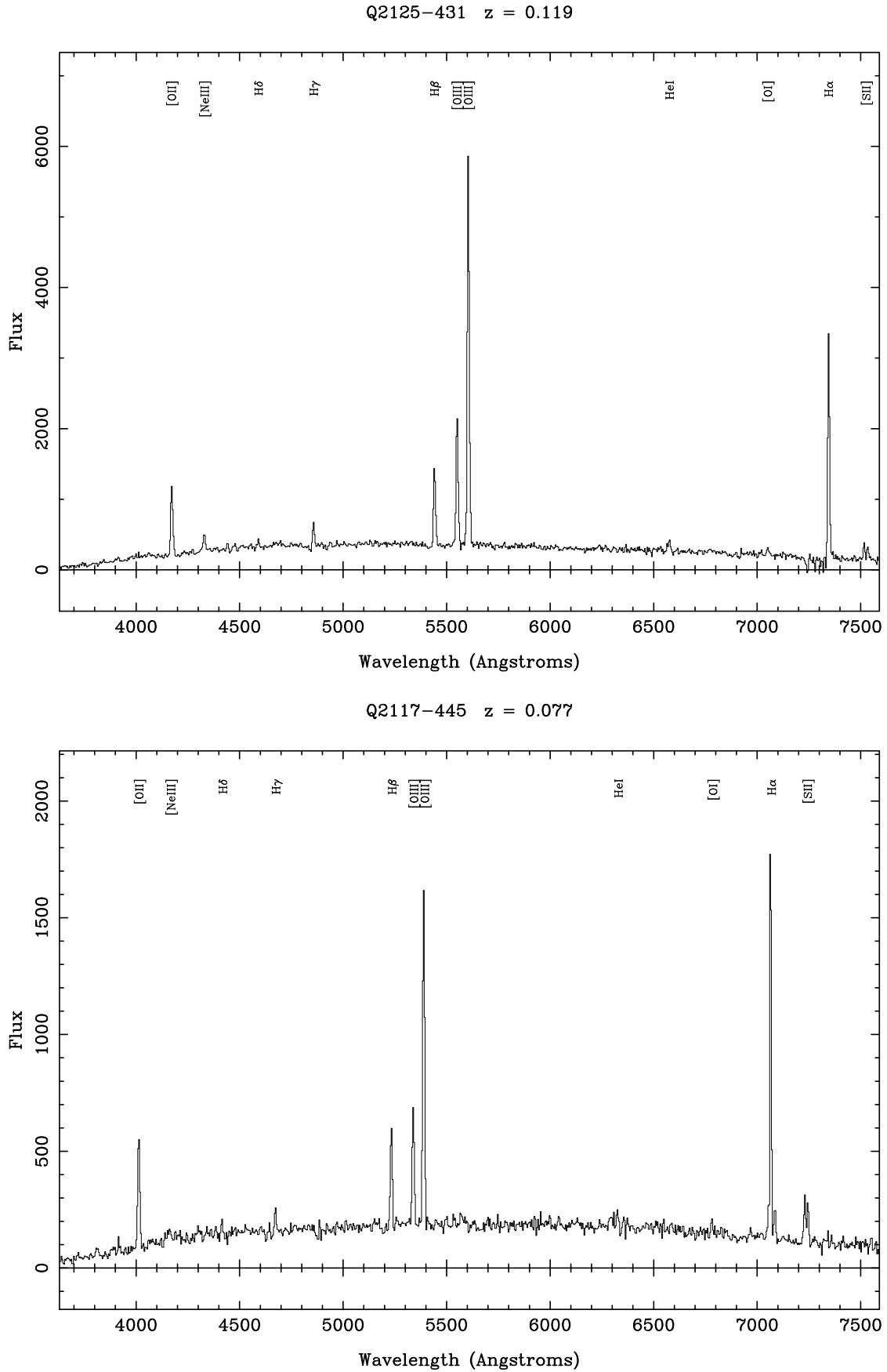


**Fig. 3.** Spectra of typical Seyfert 2 or starburst galaxies (flux in arbitrary units).

**Table 1.** Seyfert galaxy line widths ( $\text{km s}^{-1}$ )

| RA (1950) |    |       | Dec (1950) |    |      | z     | $\delta B$ | [O II] | [Ne III] | H $\beta$ | [O III] | [O III] | H $\alpha$ | O/H   |
|-----------|----|-------|------------|----|------|-------|------------|--------|----------|-----------|---------|---------|------------|-------|
| 21        | 17 | 36.57 | -44        | 36 | 49.0 | 0.391 | 0.71       | 1117   | 1058     | 1802      | 892     | 850     | 0          | 2.89  |
| 21        | 17 | 53.12 | -44        | 32 | 6.9  | 0.077 | 0.24       | 972    | 0        | 670       | 714     | 643     | 471        | 3.23  |
| 21        | 17 | 55.10 | -44        | 46 | 33.3 | 0.175 | 0.19       | 943    | 0        | 691       | 687     | 626     | 378        | 2.86  |
| 21        | 18 | 21.53 | -44        | 44 | 25.7 | 0.365 | 0.50       | 989    | 765      | 3246      | 792     | 717     | 0          | 2.29  |
| 21        | 18 | 24.15 | -45        | 11 | 18.1 | 0.272 | 0.29       | 899    | 813      | 642       | 557     | 557     | 0          | 4.64  |
| 21        | 19 | 48.47 | -43        | 57 | 2.2  | 0.092 | 0.24       | 927    | 745      | 699       | 627     | 550     | 369        | 4.01  |
| 21        | 20 | 40.52 | -45        | 48 | 52.1 | 0.128 | 0.29       | 1202   | 0        | 761       | 704     | 614     | 508        | 3.17  |
| 21        | 22 | 49.22 | -44        | 24 | 19.4 | 0.311 | 0.92       | 790    | 0        | 351       | 714     | 699     | 0          | 5.89  |
| 21        | 23 | 31.47 | -42        | 56 | 35.7 | 0.141 | 1.26       | 973    | 0        | 553       | 301     | 696     | 429        | 1.55  |
| 21        | 23 | 34.42 | -43        | 38 | 39.1 | 0.469 | 0.19       | 983    | 0        | 738       | 998     | 531     | 0          | 0.81  |
| 21        | 23 | 46.41 | -42        | 55 | 54.5 | 0.250 | 0.43       | 860    | 0        | 560       | 528     | 531     | 0          | 3.98  |
| 21        | 24 | 18.01 | -43        | 49 | 22.9 | 0.294 | 0.24       | 863    | 468      | 657       | 563     | 555     | 0          | 1.45  |
| 21        | 24 | 22.46 | -42        | 59 | 37.9 | 0.179 | 0.16       | 976    | 0        | 628       | 497     | 696     | 0          | 4.41  |
| 21        | 24 | 24.99 | -42        | 51 | 51.5 | 0.099 | 0.61       | 851    | 0        | 1049      | 862     | 703     | 456        | 1.67  |
| 21        | 24 | 54.69 | -45        | 4  | 54.4 | 0.388 | 0.32       | 989    | 0        | 584       | 629     | 680     | 0          | 2.09  |
| 21        | 25 | 50.21 | -43        | 39 | 8.0  | 0.252 | 0.19       | 889    | 981      | 612       | 661     | 572     | 0          | 2.89  |
| 21        | 25 | 54.29 | -43        | 8  | 56.7 | 0.119 | 0.27       | 986    | 1103     | 721       | 623     | 666     | 452        | 4.53  |
| 21        | 26 | 10.02 | -42        | 56 | 30.8 | 0.410 | 0.74       | 1034   | 1375     | 3819      | 1040    | 1052    | 0          | 0.55  |
| 21        | 26 | 30.00 | -42        | 47 | 44.8 | 0.291 | 0.43       | 982    | 0        | 694       | 682     | 652     | 0          | 2.55  |
| 21        | 26 | 48.98 | -43        | 44 | 12.9 | 0.481 | 0.76       | 1086   | 985      | 834       | 786     | 772     | 0          | 10.83 |
| 21        | 26 | 51.91 | -42        | 46 | 0.8  | 0.333 | 0.59       | 884    | 0        | 2040      | 815     | 782     | 0          | 1.31  |
| 21        | 26 | 52.50 | -44        | 23 | 42.9 | 0.230 | 0.25       | 880    | 1070     | 590       | 524     | 494     | 0          | 3.97  |
| 21        | 27 | 10.40 | -42        | 52 | 58.3 | 0.158 | 0.14       | 804    | 920      | 605       | 609     | 600     | 0          | 2.65  |
| 21        | 27 | 22.15 | -43        | 54 | 7.8  | 0.188 | 0.20       | 1002   | 1698     | 674       | 689     | 660     | 475        | 3.82  |
| 21        | 27 | 28.22 | -43        | 20 | 3.5  | 0.017 | 0.19       | 1090   | 0        | 673       | 664     | 666     | 502        | 3.14  |
| 21        | 27 | 33.98 | -44        | 39 | 18.9 | 0.481 | 1.14       | 1012   | 1062     | 1676      | 701     | 746     | 0          | 4.65  |
| 21        | 28 | 24.69 | -45        | 37 | 3.4  | 0.202 | 0.74       | 1133   | 0        | 3744      | 670     | 558     | 1995       | 0.40  |
| 21        | 29 | 5.73  | -46        | 24 | 19.9 | 0.140 | 0.15       | 746    | 1822     | 575       | 584     | 594     | 446        | 2.16  |
| 21        | 29 | 9.29  | -44        | 15 | 7.9  | 0.267 | 0.56       | 1341   | 1264     | 6239      | 1025    | 1116    | 0          | 2.28  |
| 21        | 29 | 19.60 | -42        | 48 | 8.8  | 0.193 | 0.79       | 0      | 0        | 2395      | 637     | 595     | 1911       | 0.41  |
| 21        | 29 | 58.80 | -42        | 49 | 26.0 | 0.194 | 0.23       | 884    | 803      | 541       | 557     | 508     | 463        | 4.35  |
| 21        | 30 | 4.24  | -43        | 7  | 44.2 | 0.266 | 1.20       | 677    | 906      | 426       | 652     | 661     | 0          | 16.36 |
| 21        | 30 | 7.17  | -43        | 25 | 42.9 | 0.456 | 1.17       | 1516   | 0        | 1637      | 1732    | 1893    | 0          | 20.82 |
| 21        | 30 | 34.23 | -46        | 36 | 1.2  | 0.188 | 0.21       | 861    | 967      | 571       | 545     | 537     | 522        | 4.30  |
| 21        | 30 | 35.22 | -45        | 4  | 35.8 | 0.340 | 0.47       | 790    | 0        | 538       | 595     | 654     | 0          | 0.53  |
| 21        | 30 | 38.56 | -45        | 17 | 43.7 | 0.110 | 0.31       | 790    | 1225     | 493       | 874     | 530     | 425        | 3.69  |
| 21        | 31 | 4.79  | -43        | 56 | 42.3 | 0.210 | 0.24       | 1010   | 0        | 621       | 703     | 648     | 0          | 3.59  |
| 21        | 31 | 15.03 | -43        | 3  | 32.7 | 0.196 | 0.98       | 929    | 0        | 3426      | 955     | 821     | 0          | 0.75  |
| 21        | 31 | 21.09 | -45        | 42 | 3.7  | 0.104 | 0.24       | 1037   | 975      | 589       | 563     | 594     | 446        | 4.25  |
| 21        | 31 | 15.90 | -42        | 43 | 18.9 | 0.365 | 1.18       | 1306   | 1223     | 983       | 1143    | 1095    | 0          | 7.43  |
| 21        | 31 | 21.75 | -42        | 57 | 23.2 | 0.199 | 0.82       | 984    | 0        | 535       | 621     | 721     | 770        | 4.16  |
| 21        | 31 | 44.75 | -43        | 45 | 49.0 | 0.160 | 0.34       | 836    | 2303     | 589       | 630     | 546     | 269        | 2.99  |
| 21        | 31 | 50.70 | -42        | 49 | 0.8  | 0.182 | 0.20       | 885    | 1390     | 647       | 543     | 652     | 427        | 3.25  |
| 21        | 32 | 6.07  | -43        | 5  | 25.8 | 0.283 | 0.25       | 1099   | 0        | 796       | 929     | 902     | 0          | 7.84  |
| 21        | 32 | 25.45 | -45        | 53 | 15.0 | 0.104 | 0.15       | 862    | 1169     | 628       | 505     | 657     | 431        | 3.31  |
| 21        | 32 | 26.06 | -44        | 59 | 2.6  | 0.190 | 0.43       | 1135   | 0        | 630       | 1295    | 681     | 434        | 3.83  |
| 21        | 32 | 44.01 | -45        | 54 | 16.4 | 0.388 | 0.39       | 800    | 0        | 578       | 629     | 609     | 0          | 1.96  |
| 21        | 32 | 51.48 | -46        | 41 | 5.8  | 0.353 | 0.89       | 1034   | 767      | 625       | 795     | 772     | 0          | 25.42 |
| 21        | 33 | 2.60  | -44        | 16 | 33.7 | 0.325 | 0.28       | 790    | 0        | 553       | 492     | 618     | 0          | 2.37  |
| 21        | 33 | 18.30 | -45        | 2  | 33.4 | 0.047 | 0.23       | 883    | 0        | 544       | 645     | 688     | 597        | 4.75  |
| 21        | 33 | 15.03 | -43        | 30 | 29.5 | 0.176 | 0.14       | 827    | 1304     | 586       | 636     | 590     | 486        | 4.04  |
| 21        | 34 | 0.20  | -45        | 27 | 9.4  | 0.136 | 0.96       | 691    | 0        | 5772      | 717     | 690     | 3517       | 0.58  |
| 21        | 34 | 48.23 | -44        | 28 | 8.1  | 0.494 | 0.52       | 888    | 0        | 613       | 919     | 969     | 0          | 2.52  |
| 21        | 35 | 0.77  | -44        | 16 | 28.6 | 0.284 | 0.22       | 951    | 1093     | 591       | 506     | 584     | 0          | 2.15  |
| 21        | 35 | 53.01 | -44        | 21 | 44.3 | 0.407 | 0.76       | 1228   | 1032     | 1498      | 825     | 884     | 0          | 0.91  |
| 21        | 35 | 54.17 | -44        | 14 | 32.4 | 0.411 | 0.19       | 970    | 760      | 515       | 714     | 629     | 0          | 5.15  |
| 21        | 36 | 3.46  | -45        | 14 | 35.3 | 0.103 | 0.29       | 874    | 0        | 491       | 559     | 572     | 518        | 6.52  |
| 21        | 36 | 31.16 | -44        | 20 | 53.9 | 0.432 | 0.26       | 984    | 0        | 546       | 693     | 731     | 0          | 1.52  |

| RA (1950) |    |       | Dec (1950) |    |      | $z$   | $\delta B$ | [O II] | [Ne III] | H $\beta$ | [O III] | [O III] | H $\alpha$ | O/H  |
|-----------|----|-------|------------|----|------|-------|------------|--------|----------|-----------|---------|---------|------------|------|
| 21        | 36 | 49.17 | -44        | 20 | 47.4 | 0.274 | 0.35       | 870    | 914      | 602       | 623     | 616     | 369        | 3.37 |
| 21        | 37 | 17.79 | -44        | 21 | 10.6 | 0.346 | 1.63       | 1022   | 690      | 637       | 929     | 741     | 0          | 3.74 |
| 21        | 37 | 24.65 | -44        | 27 | 28.9 | 0.108 | 0.51       | 796    | 0        | 465       | 510     | 533     | 442        | 1.82 |
| 21        | 37 | 56.97 | -44        | 45 | 33.4 | 0.269 | 0.26       | 994    | 3513     | 668       | 878     | 699     | 0          | 2.95 |
| 21        | 37 | 57.13 | -44        | 44 | 29.1 | 0.356 | 0.61       | 832    | 1523     | 3048      | 665     | 789     | 0          | 1.18 |
| 21        | 37 | 56.15 | -44        | 34 | 26.2 | 0.141 | 0.30       | 951    | 0        | 620       | 596     | 639     | 438        | 3.39 |
| 21        | 38 | 19.28 | -44        | 40 | 34.3 | 0.158 | 0.40       | 938    | 0        | 484       | 368     | 355     | 0          | 0.78 |
| 21        | 38 | 32.36 | -44        | 26 | 47.6 | 0.101 | 0.20       | 1082   | 0        | 577       | 641     | 636     | 468        | 3.63 |
| 21        | 39 | 6.77  | -44        | 6  | 53.2 | 0.181 | 0.15       | 908    | 1104     | 642       | 641     | 668     | 457        | 4.24 |

Of the 129 objects with  $z < 0.5$ , 37 were Seyfert 1 galaxies with broad Balmer lines and relatively narrow forbidden lines. The spectra of two of these are illustrated in Fig. 1, where the width of the permitted lines and the [O III]  $\lambda 5007$ /H $\beta$  ratio put them firmly in the Seyfert 1 domain. Among these broad line objects there were also 5 narrow-line Seyfert 1 galaxies in the sense of Osterbrock & Pogge (1985) with H $\beta$  FWHM  $\lesssim 2000$  km sec $^{-1}$  and [O III]  $\lambda 5007$ /H $\beta$   $\lesssim 3$  with S/N good enough to be confident of their classification. The spectra of two of these are shown in Fig. 2 (one with LINER characteristics), where it will be seen that the Balmer lines are weak and narrow compared with those in Fig. 1.

Spectra of the remaining 92 objects were characteristic of Seyfert 2 or starburst galaxies with narrow forbidden and permitted lines of similar width. From these, 55 were selected as having adequate signal-to-noise for further study. In all cases, narrow [O III]  $\lambda 5007$ , [O II]  $\lambda 3727$  and other forbidden lines were clearly seen, and H $\beta$  was narrow and weak, sometimes narrower than the forbidden lines. H $\alpha$  was similarly narrow where observed in the lowest redshift objects. Two typical examples are illustrated in Fig. 3, and show all the normal characteristics of Seyfert 2 galaxies. The forbidden lines include [O III]  $\lambda 5007$ , [O III]  $\lambda 4959$ , [O II]  $\lambda 3727$  [Ne III]  $\lambda 3869$ , [SII]  $\lambda 6716 + 6731$  and [OI]  $\lambda 6300$  as well as narrow Balmer lines and HeI  $\lambda 5876$ . On the basis of the spectral classification scheme of Veilleux & Osterbrock (1987) these objects lie in or near the region occupied by AGN, and are probably Seyfert 2 galaxies.

The measurement of line widths and other information for the sample of emission line galaxies is given in Table 1. The first six columns give the Right Ascension and Declination for the sample members, and the seventh column the redshift measured from the forbidden lines. Column 8 gives the amplitude in the  $B_J$  band measured over the period from 1975 to 2002 and is described further below. Columns 9 to 14 give the FWHM line widths in km sec $^{-1}$  of the [O II]  $\lambda 3727$ , [Ne III]  $\lambda 3869$ , H $\beta$   $\lambda 4861$ , [O III]  $\lambda 4959$ , [O III]  $\lambda 5007$  and H $\alpha$   $\lambda 6563$  lines, measured as described above. No attempt has been made to correct the line widths for instrumental broadening, and given the estimated spectral resolution from the night sky lines, many of the forbidden lines are effectively unresolved. In cases where the line is redshifted out of the observed passband, or is not seen in the spectrum a value of zero is given. The final column is the [O III]  $\lambda 5007$ /H $\beta$  line strength ratio which is commonly used as a discriminant between various classes of active galaxies. There is for the most part a good correlation between the [O III]  $\lambda 5007$  and [O III]  $\lambda 4959$  line widths, giving additional support to the error estimates discussed above. The [O II]  $\lambda 3727$  line tends to be of similar or greater width than the [O III] lines

### 2.3. Light curves

The quasar monitoring programme in field 287 was started in 1975, and between 1977 and 2002 at least one and usually 4 plates in the  $B_J$  passband (IIIa-J emulsion though a GG395 filter) have been taken each year (see Hawkins (2003) for details). The primary purpose of these data is for Fourier analysis of the spectrum of variations, but they are also well-suited to identifying morphological features in the light curves, and measuring basic properties of the variation such as amplitude.

Fig. 4 shows the light curves of the objects with spectra in Figs 1-3. The top two panels are for Seyfert 1 galaxies, and they show variations typical for this class of object. The middle two panels are for narrow line Seyfert 1 galaxies, and they too show variations. For the left hand panel the light curve is similar to the normal Seyfert 1 galaxies, but for the right hand panel the variations are smaller and the object hardly varies significantly for most of the monitoring period. The bottom two panels show light curves for the objects classified from their spectra in Fig. 3 as Seyfert 2 or possibly starburst galaxies. It will be seen that they do not vary in brightness within the observational errors which is in line with the current understanding of the Seyfert 2 phenomenon in which the active nucleus is being viewed as weak reflected polarised light which due to its diffuse nature can only vary in brightness on very long timescales.

## 3. Naked active galactic nuclei

Perhaps the most straightforward discriminant between the various classes of AGN is the width of the Balmer lines. For normal quasars and Seyfert 1 galaxies the FWHM of these lines is typically 6000 - 10000 km sec $^{-1}$ . In the class of narrow line Seyfert 1 galaxies (NLS) defined by Osterbrock & Pogge (1985) it is usually less than 2000 km sec $^{-1}$ , and often only slightly larger

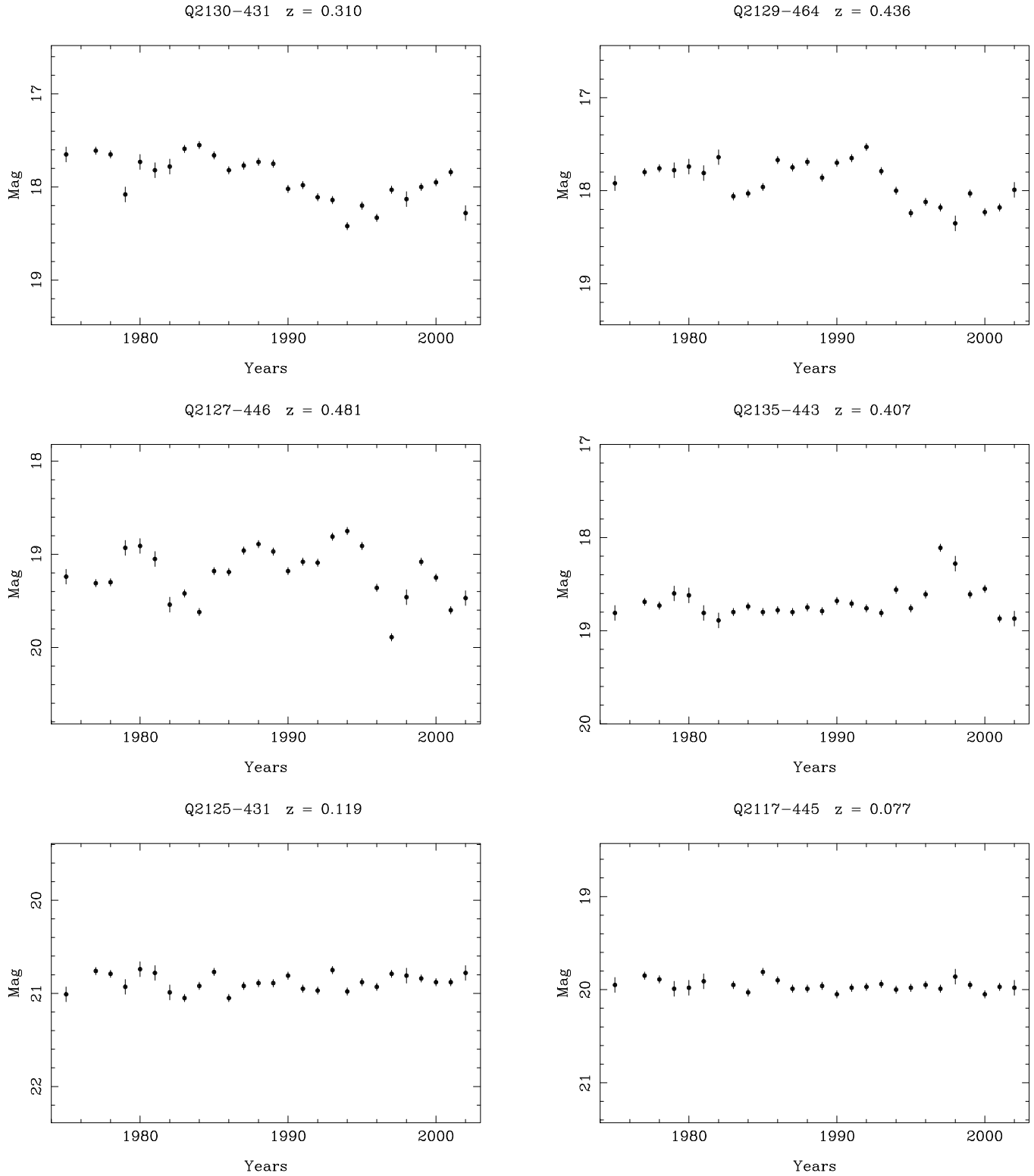


**Fig. 4.** Light curves for Seyfert galaxies in the  $B_J$  passband. The top two panels are for Seyfert 1 galaxies, the middle two for narrow line Seyfert 1 and the bottom two for Seyfert 2 or starburst galaxies.

than the forbidden line widths. Another important defining characteristic of Seyfert galaxies is the  $[\text{O III}] \lambda 5007/\text{H}\beta$  line strength ratio which is used to distinguish between Seyfert 1 and Seyfert 2 galaxies (Shuder & Osterbrock 1981). In this paper they define Seyfert 2 galaxies as having  $[\text{O III}] \lambda 5007/\text{H}\beta > 3$ , a definition which has stood the test of time in subsequent studies (Rodríguez-Ardila et al. 2000). The  $[\text{O III}] \lambda 5007/\text{H}\beta$  has also proved useful in distinguishing between Seyfert 2 galaxies and H II region-like or starburst galaxies, where a high values favours a Seyfert 2 classification (Veilleux & Osterbrock 1987).



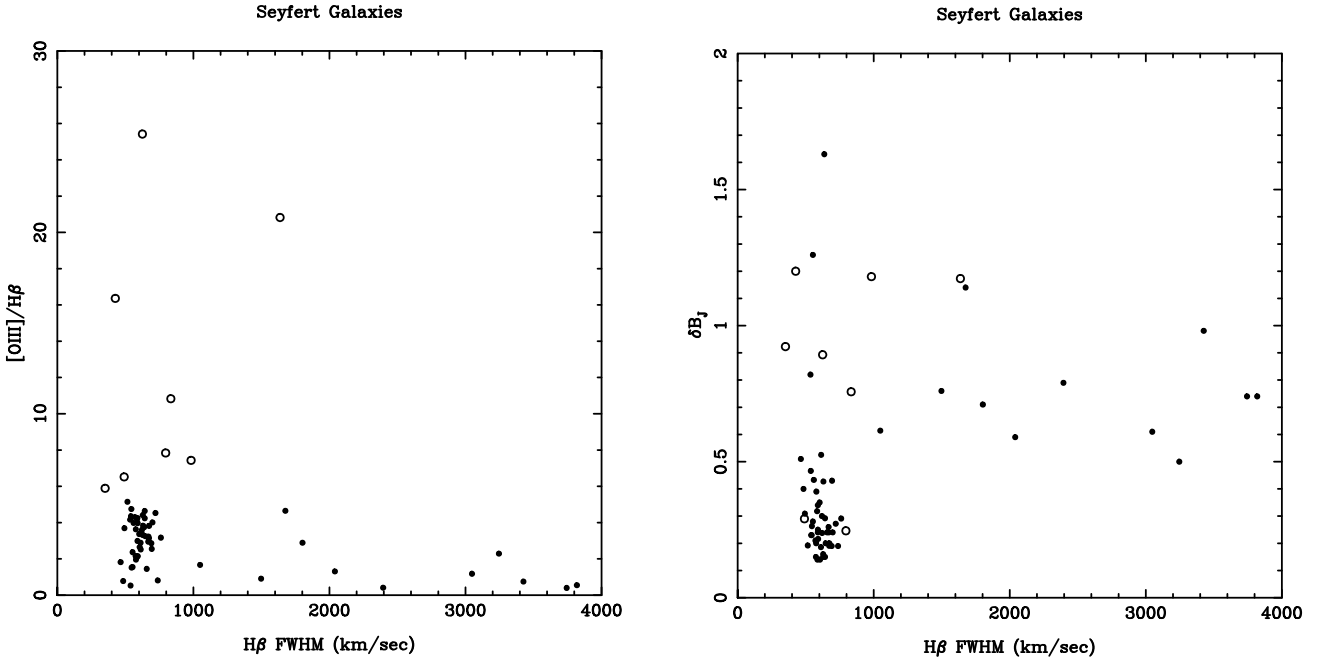


**Fig. 5.** Relation between  $H\beta$  line width and  $[O\ III]\ \lambda 5007/H\beta$  line strength ratio (left hand panel) and between  $H\beta$  line width and amplitude (right hand panel). Objects with the largest  $[O\ III]\ \lambda 5007/H\beta$  ratio are shown as open circles.

In Fig. 5 (left hand panel) we plot the relationship between  $H\beta$  line width and  $[O\ III]\ \lambda 5007/H\beta$  line strength ratio. The diagram may be divided into three zones. Firstly, Seyfert 1 type galaxies or quasars may be seen along the bottom with  $[O\ III]\ \lambda 5007/H\beta < 3$  in all but one case, and a broad Balmer line ( $H\beta$  FWHM  $> 1000\text{ km sec}^{-1}$ ). In the bottom left hand corner there is a compact group of objects with small  $[O\ III]\ \lambda 5007/H\beta$  and small  $H\beta$  FWHM which is the area occupied by starburst and some Seyfert 2 galaxies. However, for the most part Seyfert 2 galaxies have larger  $[O\ III]\ \lambda 5007/H\beta$  (Veilleux & Osterbrock 1987) and such objects may be seen in the left hand side of the diagram. These galaxies form a well defined group in Fig. 5, and have been plotted as open circles. On the basis of their large  $[O\ III]\ \lambda 5007/H\beta$  ratio and small  $H\beta$  FWHM these objects are most likely to be Seyfert 2 galaxies, or possibly starburst galaxies. Either way they should definitely not vary in optical passbands.

The right hand panel of Fig. 5 shows the same objects, but this time with amplitude plotted as a function of  $H\beta$  line width. The amplitude is taken from the monitoring programme described above, and is the difference between maximum and minimum light in magnitudes in the  $B_J$  passband over a period of 27 years. In this diagram, the objects with large  $H\beta$  line width identified as quasars all appear with amplitudes of 0.5 magnitudes or more, as expected for quasars (Hawkins 2000). Most of the objects in the bottom left of the left hand panel classified as Seyfert 2 or starburst galaxies show little or no significant variation, but six of the eight objects with large  $[O\ III]\ \lambda 5007/H\beta$  shown as open circles have the large amplitude normally only found for quasars or Seyfert 1 galaxies. In fact in the right hand panel of Fig. 5 they seem to form a natural extension of the quasar locus into the small  $H\beta$  line width regime.

In Figs 6 and 7 we show the spectra of four of the large amplitude objects shown as open circles in Fig. 5. All four spectra show very weak  $H\beta$  of a similar or smaller FWHM to the forbidden lines, and in each case there is no sign of a broad component to the line. This is very characteristic of Seyfert 2 galaxies, although does not absolutely exclude starburst galaxies (Veilleux & Osterbrock 1987). The strength of  $[SII](\lambda 6716 + \lambda 6731)$  or  $[OI]\lambda 6300$  would settle the matter, but unfortunately in all four cases they are redshifted out of the optical passband. All four spectra show strong narrow forbidden lines of  $[O\ III]\ \lambda 5007$   $[O\ III]\ \lambda 4959$  and  $[O\ II]\ \lambda 3727$ , and in three cases  $[Ne\ III]\ \lambda 3869$ . There is good agreement between the FWHM of the two  $[O\ III]$  lines, but the  $[O\ II]$  and  $[Ne\ III]$  lines tend to be somewhat broader. The  $H\beta$  line on the other hand is very weak and tends to be narrower than the forbidden lines. Other Balmer lines and the  $Mg\ II\ \lambda 2798$  line are not detected.

On the face of it, the four objects in Figs 6 and 7 have spectra indistinguishable from Seyfert 2 galaxies. However their place among the six large amplitude objects shown as open circles in the right hand panel of Fig. 5 would appear to rule out this classification, or indeed that of starburst galaxy. To illustrate the nature of their variability better, their light curves are shown in the top four panels of Fig. 8. It will be seen that all four objects show brightness variations by a factor of 3 or more on a timescale of 5 to 10 years as well as shorter term variations. This type of variation implies a direct view of the compact nucleus itself. Such strong rapid variability could not be seen in the weak reflected light which is supposed to characterise a Seyfert 2 nucleus. Furthermore, the strong variations in nuclear light can be used to put a lower limit on the luminosity of the nucleus. On the basis that the change in flux can only be due to the nuclear light, then at maximum the absolute magnitudes of the nuclei turn

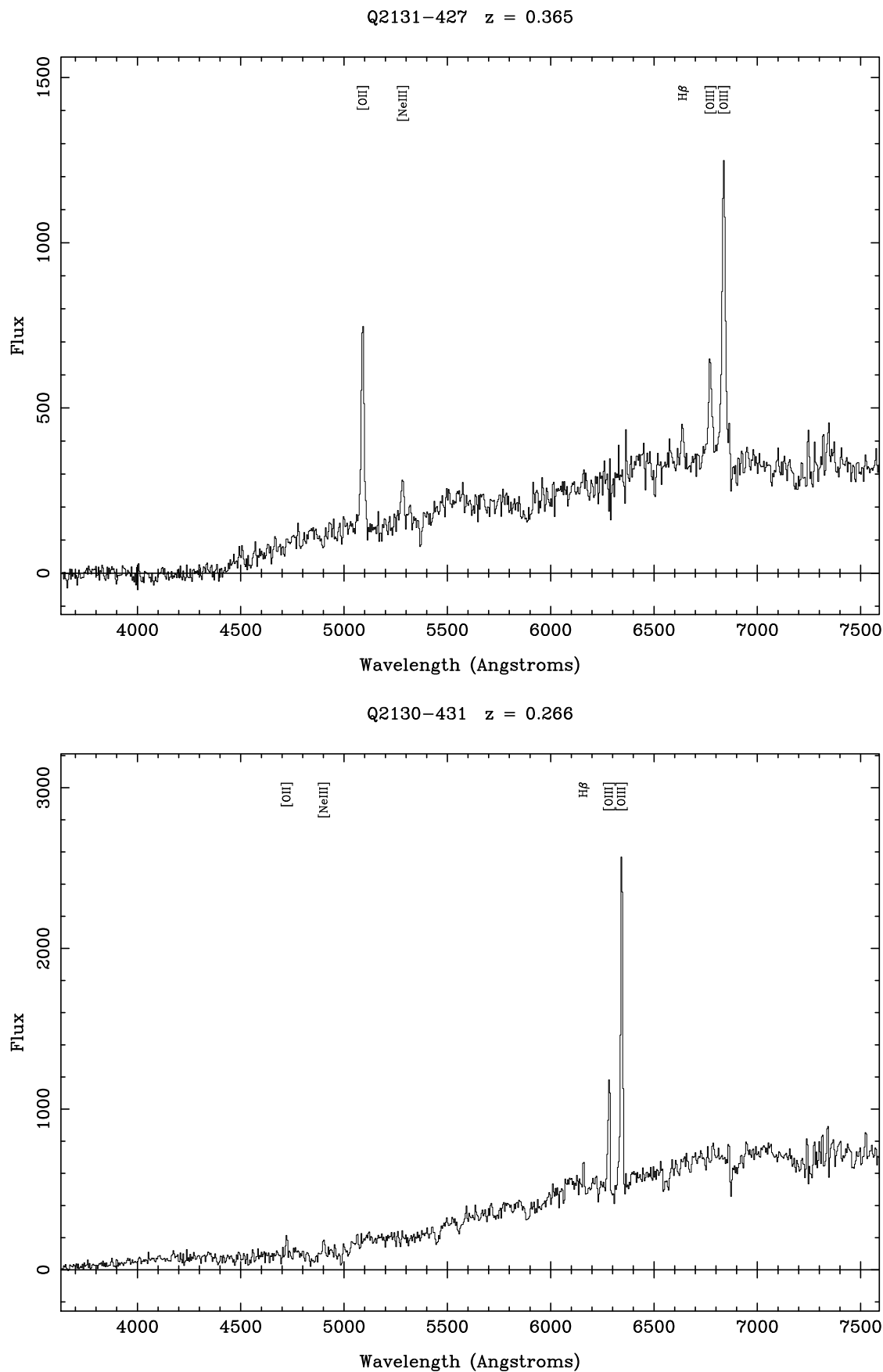


**Fig. 6.** Spectra of variable Seyfert galaxies with Seyfert 2 type spectra (flux in arbitrary units).

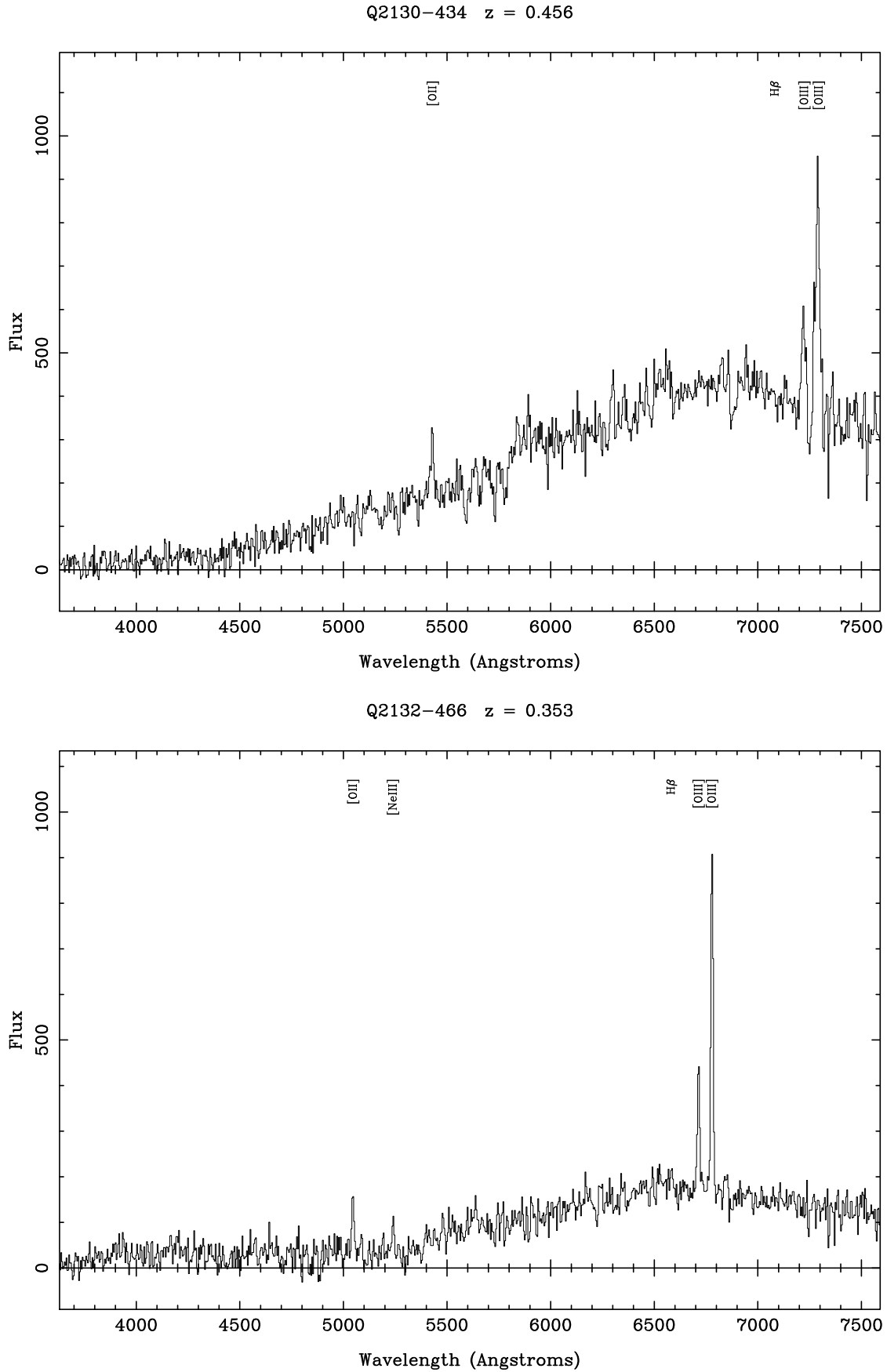


**Fig. 7.** Spectra of variable Seyfert galaxies with Seyfert 2 type spectra (flux in arbitrary units).

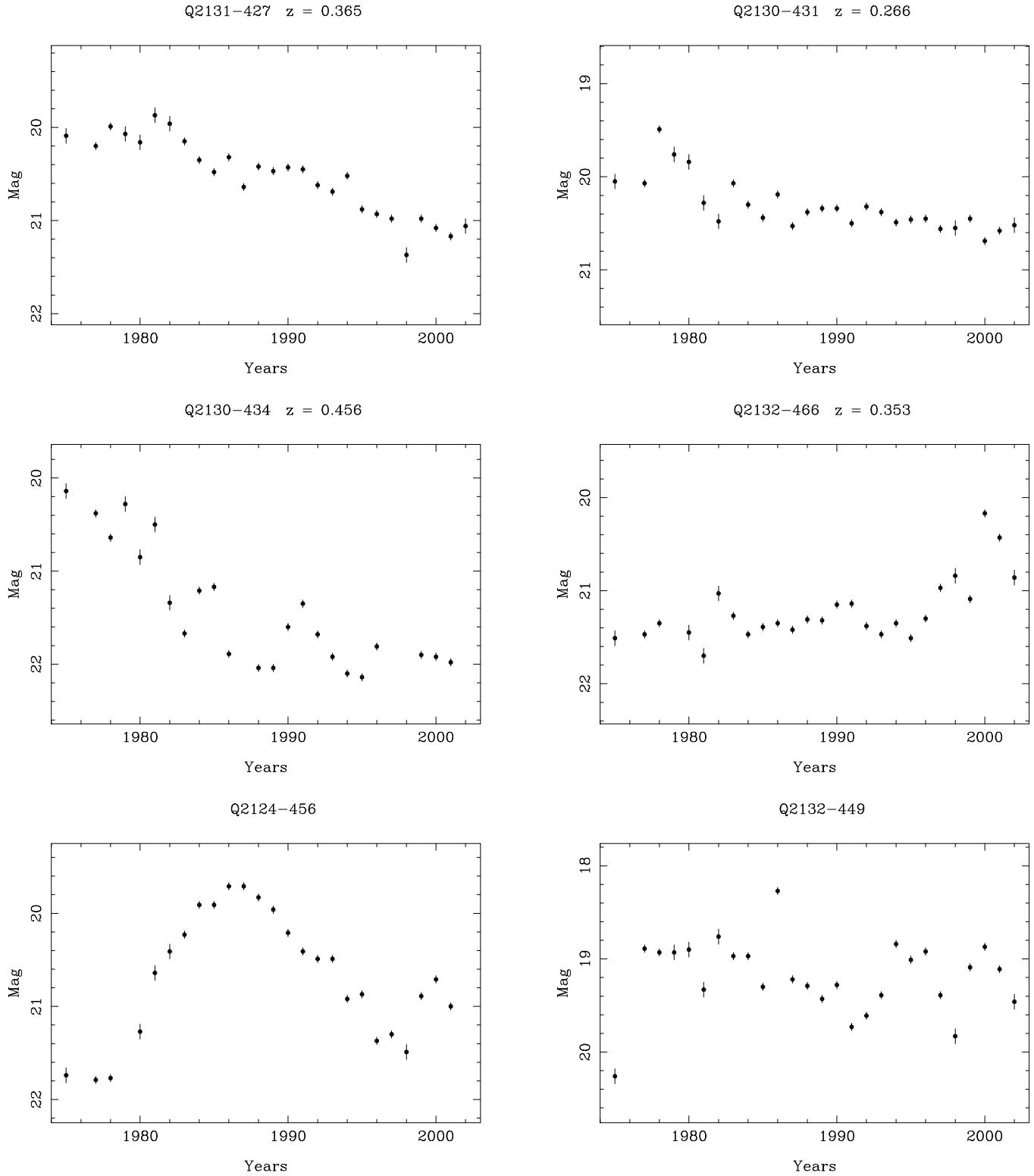


**Fig. 8.** Light curves for active galaxies in the  $B_J$  passband. The top four panels are for galaxies with Seyfert 2 type spectra, and the bottom two for galaxies with featureless spectra.

out to be  $M_B \leq -21.5$ . This figure, which by the nature of the derivation excludes any contribution from the underlying galaxy, is typical for Seyfert 1 galaxies. However, it is very much greater than for Seyfert 2 galaxies where for example in the well-studied (Crenshaw & Kraemer 2000) and archetypal NGC 1068 the continuum emission amounts to a luminosity of  $M_B \approx -15.3$ .

For objects with luminous variable nuclei, the unified model of AGN would lead one to expect a spectrum dominated by broad emission lines. In particular, at this redshift one would expect to see strong broad  $H\beta$ ,  $H\gamma$ ,  $H\delta$  and  $Mg II$  emission lines as

seen for example in Figs 1 and 2. As discussed above, the spectra shown in Figs 6 and 7 have all the characteristics of Seyfert 2 spectra. The  $H\beta$  lines are weak and narrow (see Table 1), and show no sign of a broad component. There are several forbidden lines in the spectra, all of a similar width or broader than the  $H\beta$  line, and the  $[O III] \lambda 5007/H\beta$  ratios put them in the domain of Seyfert 2 galaxies (Veilleux & Osterbrock 1987), and certainly outside the parameter space occupied even by narrow line Seyfert 1 galaxies (Osterbrock & Pogge 1985). However, the luminosity and variability of the nuclei make it clear that we are not viewing a Seyfert 2 galaxy. The only plausible explanation appears to be that these are AGN without a broad line region.

#### 4. Discussion

One possible explanation for the absence of broad emission lines in AGN spectra is that they fade in response to decrease in the continuum flux. Although it is hard to rule this possibility out, it can be checked for Q2131-427 for which an earlier spectrum exists. This object was observed in 1991 with EFOSC on the 3.6m at ESO as part of an earlier follow-up to the monitoring programme. It will be seen from Fig. 8 that at that time it was 0.7 magnitudes brighter than in 2002 when the spectrum in Fig. 6 was obtained. The early spectrum is however essentially unchanged apart from additional flux at the blue end of the continuum. There is still no sign of any broad emission lines, and the  $H\beta$  line is narrow and weak as in Fig. 6.

Another possibility is that the spectra in Figs 6 and 7 show Seyfert 1.8 or 1.9 galaxies in a low state. These galaxies, first described by Osterbrock (1981), have a weak or undetectable broad component to the  $H\beta$  line but broad  $H\alpha$  emission. These galaxies are known to vary between this state and a more normal Seyfert 1 type spectrum, and a case has been made by Goodrich (1989) that this change is due to variable reddening. To test this mechanism for the objects in our sample we have simulated the effect of reddening a Seyfert 1 type spectrum to the point where the broad  $H\beta$  line becomes washed out in the spectrum of the underlying galaxy to determine whether the blue continuum is still detectable. For a model quasar spectrum we used the composite from the FIRST bright quasar survey (Brotherton et al. 2001), and for the underlying galaxy the models of Jimenez et al. (2004). The top panel of Fig. 9 shows the combined quasar and galaxy spectrum as a solid line, and the galaxy contribution as a dashed line. In the bottom panel the quasar spectrum has been reddened to the extent that the broad  $H\beta$  line is no longer visible, which results in the continuum emission being extinguished to the extent that it is small compared with the galaxy light, and insufficient to cause significant variation of the combined flux.

A feature of Seyfert 1.8 and 1.9 Seyfert galaxies is that even when the broad  $H\beta$  line is washed out, the broad  $H\alpha$  line remains relatively strong and clearly visible (Osterbrock 1981). Although the objects in Figs 6 and 7 are at too high a redshift to observe the  $H\alpha$  line in the optical, there is one variable AGN in the sample at a sufficiently low redshift to test for a broad  $H\alpha$  component. This object was not included in the sample of naked AGN candidates as the signal-to-noise of the spectrum is rather poor, but it is sufficiently good to throw some light on the presence of a broad  $H\alpha$  line. The spectrum is shown in Fig. 10, and it will be seen that both the  $H\alpha$  and  $H\beta$  lines are narrow, of comparable width to the forbidden lines, and in neither case is there any indication of the presence of a broad component.

The broad line region has been seen as a fundamental part of the structure of AGN, although the unified model explains its presence rather than providing a compelling argument for its existence. It is now clear that in a significant fraction of AGN the broad line region is not present. Although there has been much debate over the structure of the BLR, there seems little doubt that it involves an interaction between the central accretion disc and a surrounding star cluster (Williams et al. 1999). The idea is that gas from the cluster falls onto the accretion disc causing a complex and unstable high velocity flow pattern in which the inflowing material is eventually accreted onto the central black hole or ejected as bi-polar winds. This high velocity turbulent gas is ionised by radiation from the accretion disc, resulting in the broad line emission. Williams et al. (1999) make the case that given inflowing material, this picture is virtually inevitable. On this basis it would thus appear that for those AGN where broad emission lines are not present, the source of inflowing material has dried up. These naked AGN therefore would represent a period in the duty cycle intermediate between activity and dormancy. They would survive on the fuel reserves present in the accretion disc.

Such ‘naked’ AGN appear to be quite common, comprising roughly 10% of the sample of the emission line galaxies observed, the remainder being Seyfert 1 galaxies with broad permitted lines, or non-variable objects with Seyfert 2 type spectra, which are presumably normal Seyfert 2 galaxies or starburst galaxies.

An interesting question which arises concerns the possibility that naked nuclei may be found among more luminous AGN in the quasar regime. This almost inevitably means that candidate objects will be at higher redshift, and much more difficult to identify without the help of a system of strong narrow forbidden lines. There is much anecdotal evidence from surveys based on UVX selection for objects with featureless spectra for which there is no plausible classification. Such objects are typically ignored for lack of observational evidence as to their nature. With information on variability, one can say a lot more. The bottom two panels of Fig. 8 show the light curves for two highly variable objects with variations characteristic of quasars (Hawkins 1996, Hawkins 2002). However, their spectra, shown in Fig. 11, are featureless. Although this is not conclusive, it is highly suggestive that we are seeing a more luminous AGN or quasar without a broad line region. It is possible that these are BL Lac objects, but such objects tend to vary more violently and on shorter timescales. Further observations including a better spectrum and polarisation measures should clarify this, but for the moment it must suffice to say that a quasar without a BLR is a plausible classification.

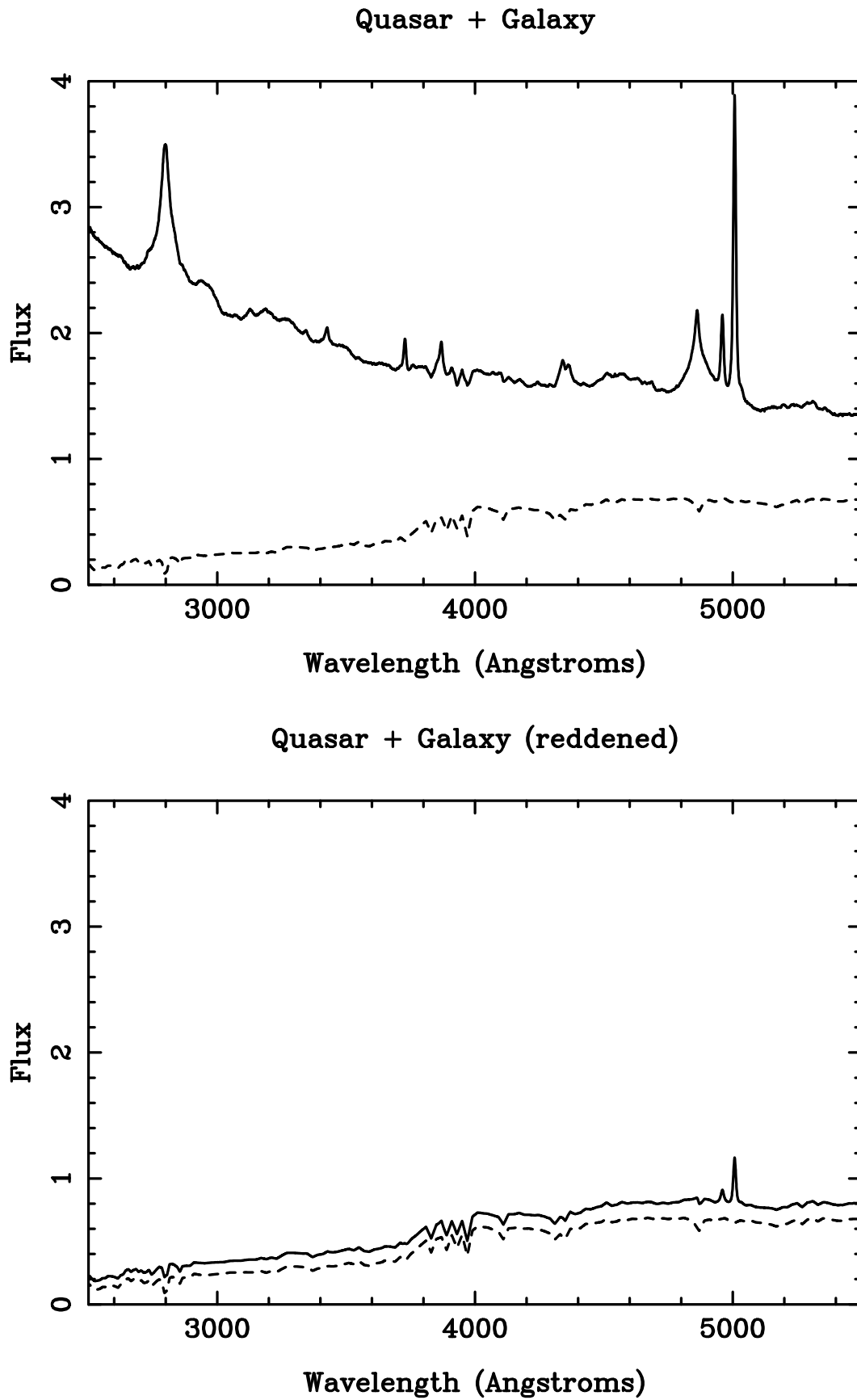


**Fig. 9.** Simulated spectra of quasar plus host galaxy (solid line) and galaxy alone (dashed line). The top panel shows the quasar spectrum unreddened, and the bottom panel with reddening sufficient to make the broad  $H\beta$  line undetectable. Flux in arbitrary units.

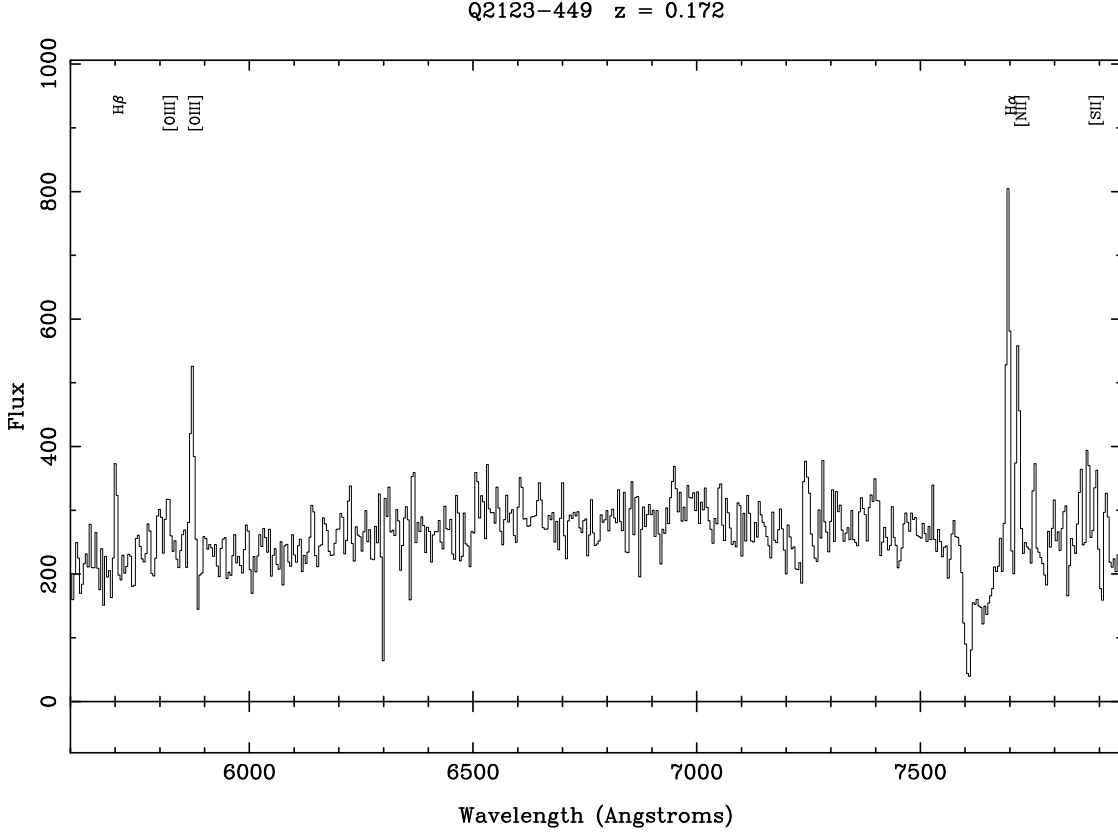


**Fig. 10.** Spectrum of a variable Seyfert galaxy showing Seyfert 2 type Balmer lines (flux in arbitrary units).

## 5. Conclusions

In this paper we have reported the discovery of a new class of AGN in which the broad emission line region is completely absent although the nucleus is viewed directly. These naked AGN were discovered as part of a survey and monitoring programme of AGN over a timescale of 25 years. Their spectra show the narrow forbidden lines characteristic of Seyfert 2 galaxies, combined with very weak narrow Balmer lines with no detectable broad component. However, The light curves show variations in brightness of at least a factor of three in all cases implying bright variable continua. We discuss other examples from the literature of AGN with weak broad emission lines, and investigate the possibility that the absence of a broad line component could be due to reddening. Our conclusion is that we are viewing the nucleus directly, and that in these AGN there is no broad line region. These objects comprise some 10% of the sample initially classified as emission line galaxies and appear to be distinct from other previously published Seyfert 1 galaxies with weak or variable emission lines. We also illustrate some possible examples of luminous AGN or quasars with no broad emission lines.

These results are discussed in the context of current models for AGN, and it is argued that the central star cluster fuelling the accretion disc has ceased supplying gas, and the naked AGN represent a transition stage between activity and a dormant phase, in which the disc draws on its internal resources to maintain its energy output.

## References

- Antonucci R., 1993, *ARA&A*, 31, 473
- Brotherton M.S. et al., 2001, *ApJ*, 546, 775
- Clavel J. et al., 1987, *ApJ*, 321, 251
- Crenshaw D.M., Kraemer S.B., 2000, *ApJ*, 532, 247–263
- Croom S.M. et al., 2002, *MNRAS*, 337, 275
- Fan X. et al., 1999, *ApJ*, 526, L57
- Goodrich R.W., 1989, *ApJ*, 340, 190
- Hawkins M.R.S., 1996, *MNRAS*, 278, 787
- Hawkins M.R.S., 2000, *A&AS*, 143, 465
- Hawkins M.R.S., 2002, *MNRAS*, 329, 76

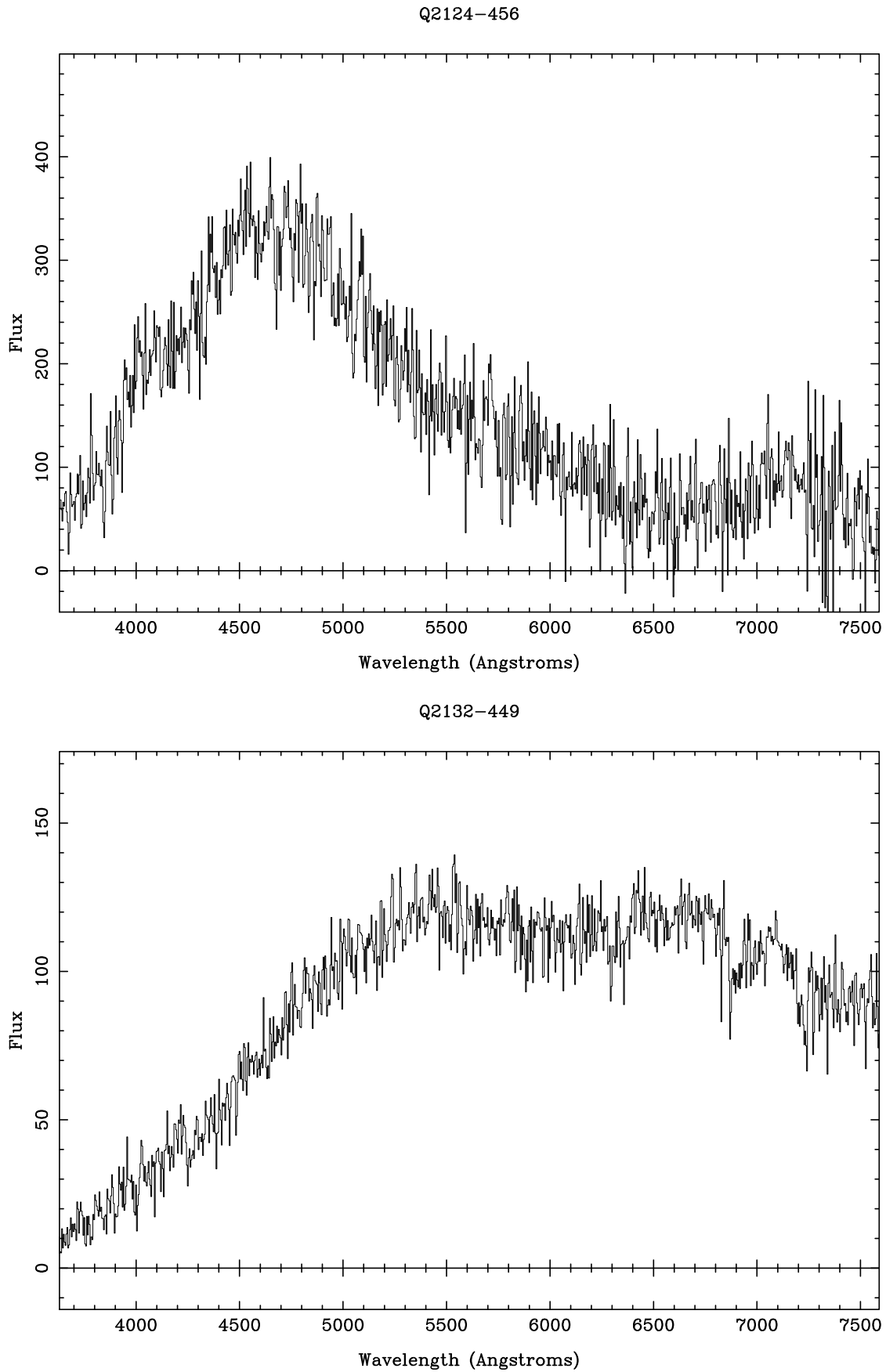


**Fig. 11.** Spectra of variable objects with featureless spectra (flux in arbitrary units).



- Hawkins M.R.S., 2003, MNRAS, 344, 492  
Jimenez R., MacDonald J., Dunlop J.S., Padoan P., Peacock J.A., 2004, MNRAS, 349, 240  
McDowell J.C., Canizaries C., Elvis M., Lawrence A., Markoff S., Mathur S., Wilkes B.J., 1995, ApJ, 450, 585  
Norman C. et al., 2002, ApJ, 571, 218  
Osterbrock D.E., 1981, ApJ, 249, 462  
Osterbrock D.E., Pogge R.W., 1985, ApJ, 297, 166  
Peterson B.M. et al., 1999, ApJ, 510, 659  
Rodríguez-Ardila A., Pastroiza M.G., Donzelli C.J., 2000, ApJS,  
Shuder J.M., Osterbrock D.E., 1981, ApJ, 250, 55  
Veilleux S., Osterbrock D.E., ApJS, 63, 295  
Williams R.J.R, 1999, MNRAS, 310, 913